The Effect of Blade Tip Geometry on the Tip Leakage Flow in Axial Turbine Cascades

F. J. G. Heyes

H. P. Hodson

Whittle Laboratory,
Cambridge University,
Cambridge CB3 ODY, United Kingdom

G. M. Dailey
Rolls Royce plc,
Derby, United Kingdom

The phenomenon of tip leakage has been studied in two linear cascades of turbine blades. The investigation includes an examination of the performance of the cascades with a variety of tip geometries. The effects of using plain tips, suction side squealers, and pressure side squealers are reported. Traverses of the exit flow field were made in order to determine the overall performance. A method of calculating the tip discharge coefficients for squealer geometries is put forward. In linking the tip discharge coefficient and cascade losses, a procedure for predicting the relative performance of tip geometries is developed. The model is used to examine the results obtained using the different tip treatments and to highlight the important aspects of the loss generation process.

Introduction

The necessary existence of a running clearance between the blade tips and casing in an unshrouded turbine is known to result in a significant loss of efficiency. Typically, a clearance gap equal to 1 percent of the blade height is associated with a 1-3 percent penalty in stage efficiency (e.g., Booth, 1985). Yet, few, if any, of the traditional correlations are based upon the physical processes involved.

There are two distinct and equally important aspects to tip leakage flows (Denton and Cumpsty, 1987). First, there is a reduction in the blade force and, therefore, the work done. This occurs because the leakage flow passes over the blade tip essentially without being turned. As a consequence of viscous effects in the tip clearance gap above the blade, entropy is also produced. The second major aspect is the subsequent mixing of the flow that has passed through the tip clearance gap with that which has passed between the blades. In linear cascade experiments, Bindon (1989) and later Dishart and Moore (1990) have shown that the loss generated by the mixing of the overtip leakage jet with the main passage flow and the loss generated in the clearance gap are approximately equal in magnitude. However, Yaras and Sjolander (1992), using a relatively thin blade at high tip clearance, have found that the gap loss is relatively small compared to the overall tip clearance loss.

Booth et al. (1982) and Wadia and Booth (1981) argued that the flow over a blade tip was analogous to that through an orifice plate. Indeed, they showed the discharge coefficients of the leakage gaps were similar to those of sharp-edged orifices. Bindon (1986) and Moore and Tilton (1988) have since shown that following the acceleration into the gap and the formation of a *vena contracta*, the flow experiences significant diffusion and mixing as it approaches the suction side of the gap. Moore and Tilton have also shown that a simple two-dimensional model can provide a reasonable description of the flow within the gap (see also Dishart and Moore, 1990).

Figure 1 illustrates the simple model of Moore and Tilton. The flow first accelerates isentropically into the vena contracta of contraction coefficient σ and then undergoes an expansion as it mixes out to uniform conditions at the tip gap exit. If there is little variation of static pressure along the blade chord, the pressure side momentum is convected through the tip gap unchanged (Rains, 1954). Hence the driving pressure for the leakage flow is the difference between the midspan static pressure on the pressure side P_P and the tip gap exit static pressure P_S, which corresponds to that on the suction side. Furthermore, if the equations for the conservation of mass and momentum are applied between the vena contracta and tip gap exit then, neglecting the effects of surface shear, the discharge coefficient may be shown to be

$$C_D = \frac{\dot{m}}{\tau\sqrt{2\rho(P_P - P_S)}} = \frac{\sigma}{\sqrt{1 - 2\sigma + 2\sigma^2}} \tag{1}$$

where $\dot{m}$ is the leakage mass flow per unit chord.

A contraction coefficient of 0.611 is obtained from a potential flow solution (Milne-Thomson, 1968) in which the static

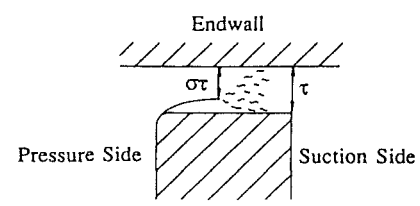

Fig. 1 Simple tip leakage flow model (after Moore and Tilton, 1988)

Contributed by the International Gas Turbine Institute and presented at the 36th International Gas Turbine and Aeroengine Congress and Exposition, Orlando, Florida, June 3-6, 1991. Manuscript received at ASME Headquarters February 20, 1991. Paper No. 91-GT-135. Associate Technical Editor: L. A. Riekert.

Table 1. Cascade geometries and test conditions

	Cascade A	Cascade B
No. of blades	7	5
Chord, c	152mm	225mm
Axial chord, c_x	110mm	103mm
Pitch/chord ratio, s/c	0.70	0.824
Aspect ratio, h/c	3.0	2.11
Reynolds No., V_2c/ν	3.15×10^5	4.0×10^5
Inlet flow angle, α_1	0°	32.5°
Blade exit angle, α_2	65°	75.6°
Max thickness/chord	20%	14%
Zweifel coefficient, Z_w	0.74	0.73

pressure is uniform across a vena contracta that forms far downstream of a sharp-edged orifice. The discharge coefficient is then equal to 0.844.

More recently Bindon and Morphis (1992) have reduced the losses generated within the tip gap by radiusing the blade pressure side tip corner, thus removing the separation bubble, and by contouring the blade tip to form, essentially, a suction side squealer. The overall losses generated within the cascade, however, were not found to be simply related to the losses generated within the gap.

The present paper is specifically concerned with the flow within the tip clearance gap and how this is modified by changes to the blade tip geometry. The results of experiments on two turbine cascades of different blade shape are reported. Each cascade was fitted with a variety of tip clearance geometries. Following a discussion of the experimental data, a potential flow/mixing model, based on that of Moore and Tilton, is proposed, which includes the effects of tip geometry. The effects of mixing are also studied using the model.

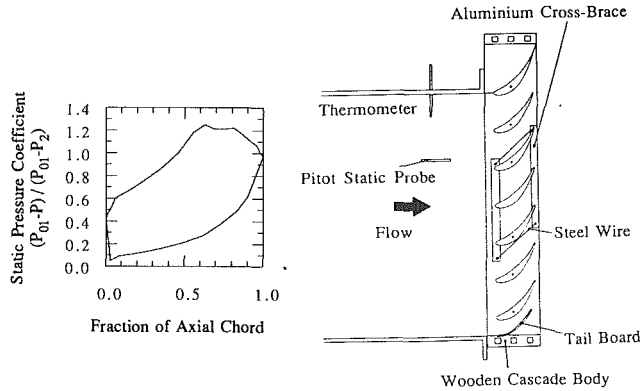

Fig. 2 General features of cascade A

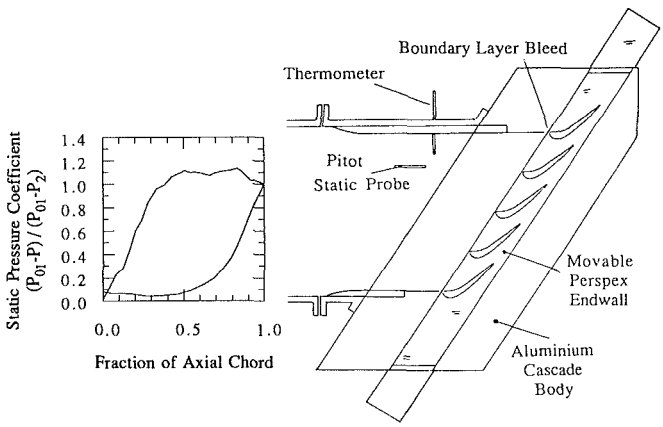

Fig. 3 General features of cascade B

Experimental Details

The Cascades. The first cascade, cascade A, has been previously used by Bindon (1986, 1989) for tip clearance studies. Table 1 gives a summary of the blade geometry and operating conditions. Figure 2 shows a schematic of the cascade and the midspan pressure distribution. Following Bindon, the tips of six of the blades were supported with threaded studs, but the central blade, behind which measurements were made, was braced between its nearest neighbors with aluminum struts. This avoided having any disturbance to the leakage flow for this blade. The profile was taken from the midspan section of a particular turbine (see Hodson, 1983), but the section is not atypical of some tip geometries.

Cascade B, shown in Fig. 3, is based upon the tip section of a model turbine that is currently under investigation. It has a larger chord than cascade A and so permits a more detailed investigation of the flow field. Despite the differences in the pressure distributions, the Zweifel coefficient for this blade is almost the same as that for cascade A. The blades were cantilevered from the aluminum "hub" endwall; this avoided the need for supporting studs and braces. Table 1 contains further information on cascade B.

Both cascades were fitted to an open jet wind tunnel so that the exhaust was at atmospheric pressure.

Instrumentation and Experimental Techniques. *Exit Traverses—Cascades A and B.* The free-stream stagnation and static pressures at inlet to the cascades were determined using an N. P. L. type Pitot static probe.

Nomenclature

c = chord
c_x = axial chord
C_D = tip discharge coefficient; see Eq. (1)
C_f = skin friction coefficient
C_P = static pressure coefficient = $(P_{01}-P)/(P_{01}-P_2)$
h = span
M = proportion of leakage mass flow mixing over the tip
P_0 = stagnation pressure
P = static pressure
s = pitch
T = tip gap length in flow direction
V = time-averaged velocity
v' = unsteady component of velocity
Z_w = Zweifel coefficient = $2\cos^2\alpha_2(\tan\alpha_2-\tan\alpha_1)\,s/c_x$
α = mainstream flow angle
θ = angle of leakage flow to mainstream
ν = kinematic viscosity
ξ = stagnation pressure loss coefficient = $(P_{01}-P_0)/(P_{01}-P_2)$
ρ = density
σ = contraction coefficient
τ = clearance between endwall and top of blade or squealer
τ_w = shear stress on the blade tip or endwall

Subscripts

b = in the tip separation bubble
e = on the cascade endwall opposite the tip separation bubble
N = velocity component normal to the blade pressure side
P = pressure side
S = suction side
1 = upstream of the cascade
2 = cascade exhaust conditions

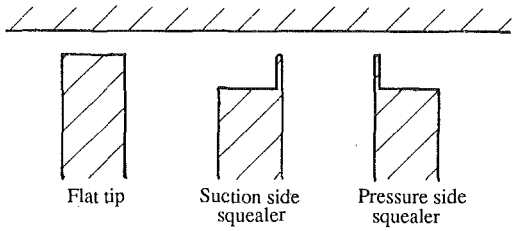

Fig. 4 Tip geometries for cascades A and B (not to scale)

The flow leaving the cascades was measured by traversing a rake of 21 Pitot tubes (spacing 3 mm) in the pitchwise direction. The measurements therefore extend from the endwall along the span to a distance of 63 mm or to 41 percent chord in the case of cascade A and 28 percent chord for cascade B. The traverses were made over one pitch. The measurements for cascade A were made at a position 1 percent chord downstream of the trailing edge, close to those of Bindon so that a direct comparison could be made. Those for cascade B were made at a more distant 12.5 percent axial chord downstream. The accuracy of the data is discussed below.

Clearance Gap Measurements—Cascade B. Measurements of the flow over the tip of the central blade of cascade B were made using a single-axis hot wire. The length of the prongs of the probe was slightly greater than the tip gap in order to prevent the stem from causing a significant blockage when fully immersed in the flow.

The measurements reported here were made on a single plane with the cascade in the flat tip configuration and at a clearance of 2.82 chord. At five axial locations and a constant pitchwise location, the hot wire was traversed in the spanwise direction. The traverse plane was located at 47 percent axial chord on the pressure side, well away from the leading edge of the blade and the effect of the inlet boundary layer. Along each traverse there were 19 spanwise stations between the endwall and the blade tip. Since the mean flow angle inside the gap was found to be in the axial direction to within 3 deg, the traverse plane is essentially a cross section through the leakage flow field.

The probe could be rotated about its spanwise axis, varying the yaw angle of the flow onto the probe. At a given probe location, velocity measurements were made over a range of angular settings. The response of the hot wire to yaw angle was symmetric about the true flow direction and approximately cosinusoidal in form. The angular settings of the probe, where the perceived velocity had decreased to half its maximum value, could be used to deduce the true flow angle. This method avoided calibrating the probe for angle variations and proved accurate in measuring the flow angle to within 2 deg. The probe was then rotated so that the axis of the wire sensor was perpendicular to the flow direction before measuring the local velocity and streamwise turbulence intensity. The axis of the wire sensor was at all times parallel to the surface of the blade tip so that no estimate of the pitchwise flow angle could be made. Allowance was made (see Hodson, 1983) for the effect of the proximity of the hot wire to the blade tip and the endwall upon the calibration of the sensor.

The velocity measurements were complemented by measurements of static pressure on the endwall and blade tip surfaces. The Perspex endwall of cascade B was fitted with a row of 19 static pressure tappings (diameter 0.2 mm). The endwall had been designed to move in a pitchwise direction so that the array of pressure tappings could be traversed across the blades to obtain a complete survey of the endwall static pressure field.

The static pressure was also measured on the blade tip surface using the "microtapping" technique of Bindon (1986). Here 17 slots were machined across the tip of the blade in a direction perpendicular to the chord line and 17 measurements were made using each slot. The minimum distance between successive tappings was 0.25 mm or 0.8 percent of the maximum blade thickness.

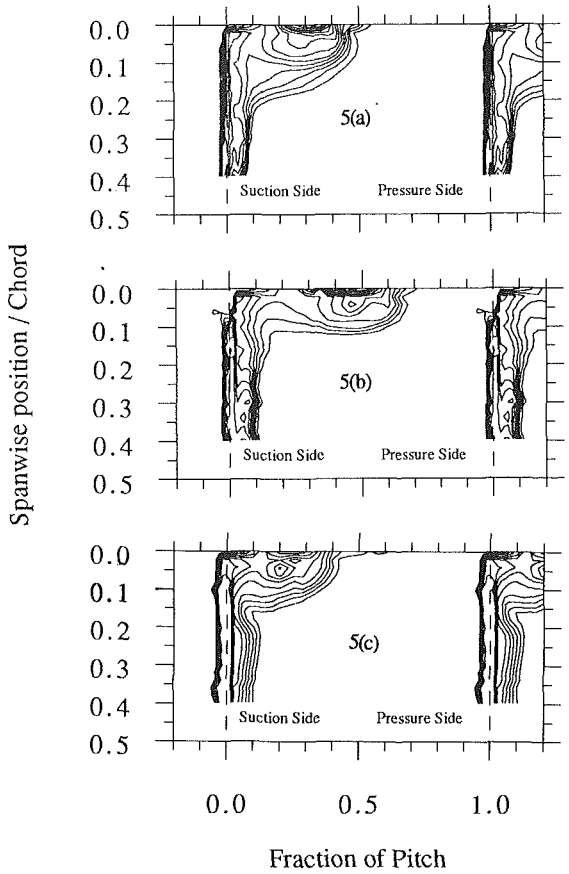

Fig. 5 Contours of stagnation pressure loss downstream of cascade A for τ/c = 1.3 percent: contour interval = 0.1 ($P_{01} - P_2$); (*a*) flat tip; (*b*) suction side squealer; (*c*) pressure side squealer

Tip Geometries. In addition to the standard flat tip configuration, the cascades were fitted with several different tip geometries for investigation. These are tabulated below and illustrated schematically in Fig. 4. The radii quoted are measured at the pressure side corner of the tip or squealer.

For the squealer geometries, results are presented for each cascade at a single tip clearance: 1.3 percent chord for cascade A and 1.0 percent chord for cascade B. Both these figures are typical of current practice.

Test Results

Cascade A. Figure 5 shows contour maps of stagnation pressure loss coefficient ξ at the exit from cascade A. Figure 5(*a*) refers to the plain cascade, Fig. 5(*b*) was obtained when the cascade was fitted with a suction side squealer, and Fig. 5(*c*) with a pressure side squealer. It should be remembered that these data were obtained just downstream of the trailing edge where the tip leakage vortex was still relatively compact. The angle of incidence of the flow onto the probes varied strongly in the measurement plane, being highest near the endwall where the tip leakage flow emerged from the blade suction side near the blade trailing edge. Flow visualization showed the incidence to be over 30 deg in this region. Although the pitot probes had an internal chamfer of 45 deg, which according to Kicks (1970) would allow an incidence of 20 deg before the probes would start to underestimate the total pressure, the results all show regions of high total pressure loss near the endwall ascribable to this phenomenon. Also, the

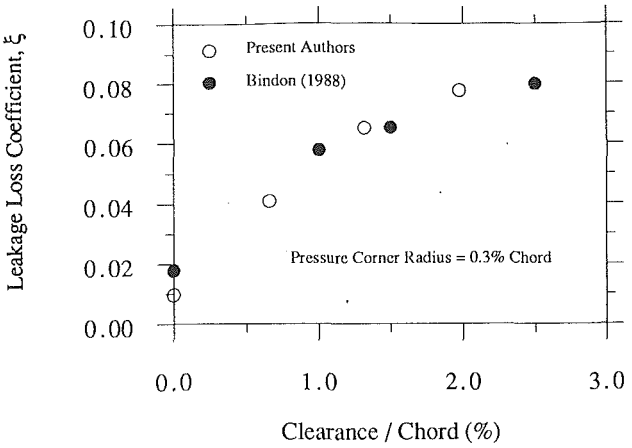

Fig. 6 Variation of loss with tip clearance for cascade A with a flat tip

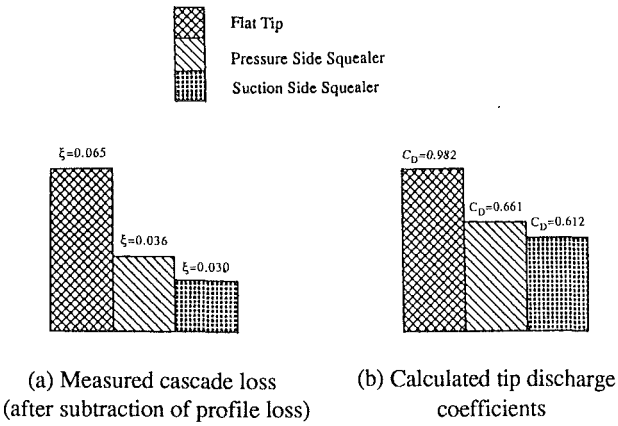

Fig. 7 Ranking of tip treatments in cascade A

flow variations in the measurement plane have yet to mix out and the loss inherent in that mixing process, attributable to the leakage flow, has not been measured by the pitot traverses. The magnitude of this mixing loss, judging by as yet unpublished five-hole probe traverses, could be as much as 30 percent of the total tip leakage loss. Since the above will be true for all the measurements behind cascade A, the close proximity of the probes to the trailing edge is not thought to affect significantly the conclusions drawn from the results.

A comparison of the plots in Fig. 5 shows that the loss core near the endwall, which is associated with the tip leakage vortex, lies at different distances from the suction side of the blade in each case. This suggests that the tip leakage flow had relatively high momentum when the suction side squealer was fitted to the cascade and had the lowest when the pressure side squealer was fitted.

A comparison of the flat tip measurements (area integrated over the measurement plane) with the three-hole probe measurements of Bindon (1989) on the same cascade is made in Fig. 6. The loss measured at a distance 41.4 percent chord from the endwall, which is taken to represent the profile loss, has been subtracted from the integrated values prior to presentation of those data so that the graph shows the variation of endwall/leakage loss with clearance. Figure 6 shows that the Pitot rake traverses give an equally adequate indication of the leakage loss as the measurements of Bindon. The profile loss was measured to be 0.035 ± 0.009, which was rather higher than the value of 0.0195 reported by Hodson and Addison (1989). However, the measurements they reported were made farther downstream of the cascade, at 50 percent axial chord, and the difference between the two sets of data is ascribed to the use of an area-averaging rather than a mass-averaging technique to determine the loss. Similarly, the variation of the present measurements of the profile loss is ascribed to small changes in the traverse plane position.

The area-integrated values of ξ for the three configurations are plotted as a histogram in Fig. 7(a). Figure 7(a) shows that for cascade A, the fitting of either the suction side or pressure side squealer provides a positive benefit with respect to the plain configuration. Also, the suction side squealer appears to be better, in terms of loss, than the pressure side squealer. However, since the measurements were made close to the trailing edge of the cascade, the apparent relative strengths of the leakage jets might result in a greater mixing loss for the suction side squealer at a plane farther downstream so that the relative merits of the suction and pressure side squealers are not necessarily clear. It should also be noted that the measurements do not give any indication of the turning afforded by the different tip geometries.

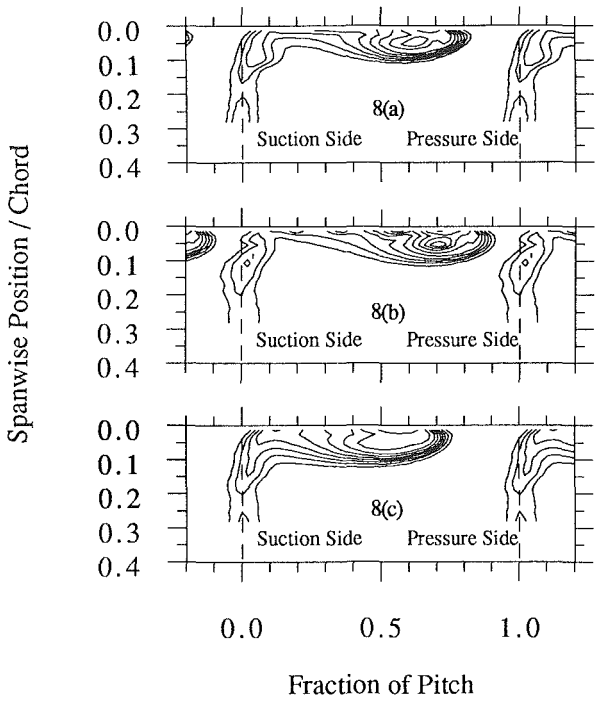

Fig. 8 Contours of stagnation pressure loss downstream of cascade B for τ/c = 1.0 percent: contour interval = 0.1 ($P_{01} - P_2$); (a) flat tip; (b) suction side squealer; (c) pressure side squealer

Cascade B. Figure 8 presents the results of the area traverses carried out downstream of the exit of cascade B using the pitot rake. The contour interval is 0.1, the same as in Fig. 5. Again the loss core for the suction side squealer is seen to be farthest from the blake wake, and that of the pressure side squealer nearest.

The integrated loss measurements for the squealer geometries, at a clearance of 1 percent chord, are again presented as a histogram in Fig. 9(a). As in the case of cascade A, it is found that the suction side squealer performs better than the pressure side squealer. However, both squealers now perform worse than the flat tip, a trend opposite to that found in cascade A. This difference between the cascades is explained below using a simple one dimensional model.

The results of the hot wire traverse in the tip gap are plotted in Fig. 10 as contours of velocity, projected onto the plane of the traverse, and the rms of the velocity perturbations (labeled "turbulence"). These perturbations include the effect of small movements in the free shear layer at the vena contracta as well as turbulence associated with mixing and boundary layers. Also

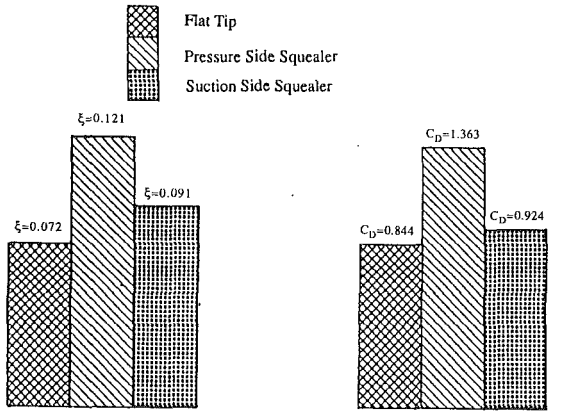

(a) Measured cascade loss (after subtraction of profile loss)

(b) Calculated tip discharge coefficients

Fig. 9 Ranking of tip treatments in cascade B

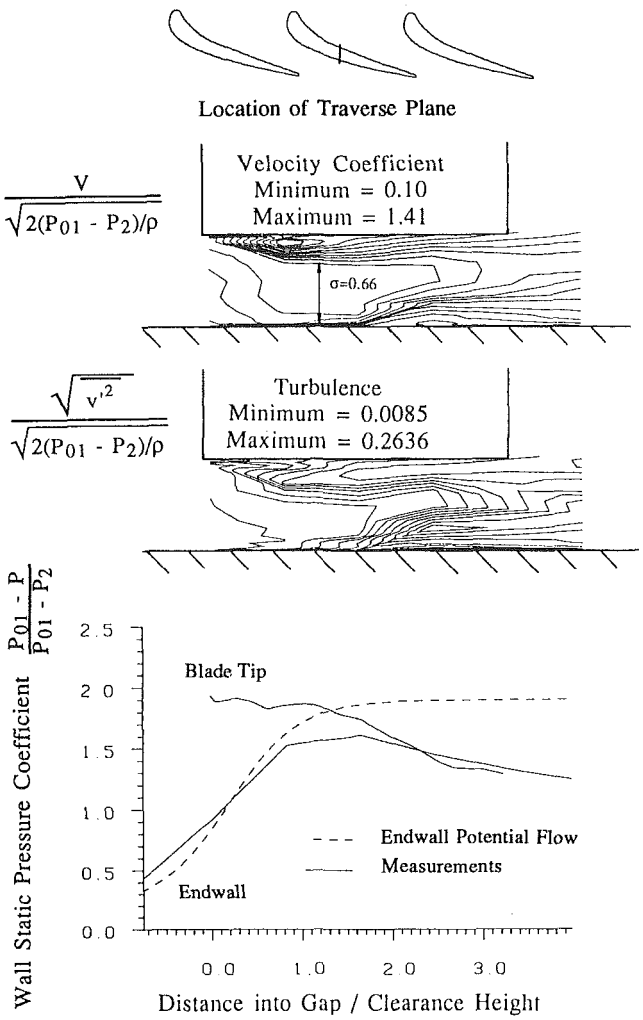

Fig. 10 Velocity and "turbulence" measurements within the clearance gap, tip and endwall surface pressure variations

presented is a plot of the variation of static pressure on the endwall and tip surfaces at the same location as the traverse plane. The clearance is 2.82 percent chord, the largest clearance investigated in cascade B. In the highly unsteady separated flow region beneath the vena contracta, the measurements obtained may be misleading. The hot wire responds only to

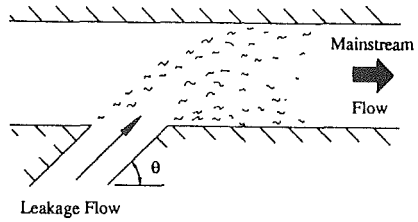

Fig. 11 The tip leakage flow modeled as an angled jet in a crossflow

the magnitude of the effective cooling velocity and not its direction. If the flow were steady, then the magnitude of the velocity would be correct, but if the flow were such that the direction was not constant, then the mean value would be overestimated.

The contours of velocity in Fig. 10 show a region of lower velocity, which extends from the pressure side corner of the tip to approximately half of the distance (1.7τ) toward the suction side of the gap. Within this separation bubble, the flow vectors no longer lie within the traverse plane, but are rotated so that there is flow along the axis of the bubble toward the trailing edge. The value of the velocity component in the traverse plane is therefore lowest near the center of this helical (Bindon, 1986) motion. The "turbulence" contours show that this region is also unsteady. This may explain why a separated shear layer does not appear to exist. The velocity is at its maximum value just outside the bubble at about 1.5 clearance heights into the gap. A contraction coefficient of 0.66 is indicated on the contours at this location. The discharge coefficient C_D, found by integration of the velocity field near gap exit, was 0.757.

The distributions of the static pressure coefficient in Fig. 10 show that the pressure on the blade tip remains approximately constant at its minimum value up to about 1.2 clearance heights into the gap, after which it rises as the separated flow begins to reattach. In contrast, the static pressure on the endwall falls up to 1.5 clearance heights into the gap after which it also rises. The static pressure on the endwall does not fall as far as that on the blade tip and the minimum value occurs later, indicating that there is curvature of the flow lines adjacent to the shear layer at the vena contracta. Moore and Tilton (1988) presented a potential flow model (after Rayleigh, 1876), which showed excellent agreement with their own endwall and blade tip static pressure data. The predictions of the same model are shown in Fig. 10; the measurements do not follow the predicted curve closely.

As the tip separation reattaches, the flow within the clearance gap decelerates and the very thin boundary layer on the endwall experiences an adverse pressure gradient. Oil flow visualization indicated that separation occurred at this point. The resulting bubble is visible in the velocity contours of Fig. 10. The highest value of "turbulence" is found over the endwall separation bubble. The mixing process, which follows the separations and is responsible for the reattachments, is also visible in the turbulence contours. The mixing regions extend across the clearance gap to affect all of the flow by 2.5 clearance heights into the gap. In contrast to the model of Moore and Tilton, but supporting Bindon's measurements in cascade A, the flow is not uniform at gap exit for this relatively large clearance.

Models of the Flow in the Tip Clearance Gap

In the succeeding paragraphs, the flow over the blade tip will be calculated by means of a one-dimensional, incompressible flow model, which follows that of Moore and Tilton (1988). The model will be used to predict qualitatively the effects of the tip clearance geometry on the total pressure losses caused by tip clearance flow.

Flat Tips. The amount of loss to be expected at the cascade exit due to leakage flow is comprised of the loss generated over the tip and that due to the mixing of the leakage flow with the mainstream. Following Denton and Cumpsty (1987), the tip leakage jet is considered to issue into the mainstream and then mix out at constant area. Here it is assumed that the leakage flow will not enter the blade passage normal to the mainstream flow but at some angle θ, as shown in Fig. 11. After Booth et al. (1982), the angle θ may be determined by assuming that the leakage velocity vector is a straight line over the tip, the component parallel to the blade pressure side being determined by the pressure side velocity, the normal component by the pressure drop across the tip, and the tip discharge coefficient. If it is also assumed that the mixing takes place at constant area, then the contribution to the overall loss of stagnation pressure due to the leakage flow across a small part of the chord, Δc, becomes

$$\Delta\xi = 2C_D L\left(\frac{\tau\Delta c}{sh\cos\alpha_2}\right)\left(1-\frac{C_D L}{\tan\theta}\right) - \left(C_D L\frac{\tau\Delta c}{sh\cos\alpha_2}\right)^2 \tag{2}$$

Here L is related to the local blade loading by the expression

$$L = \sqrt{\frac{P_p - P_s}{P_{01} - P_2}}$$

The tip clearance is small compared to the blade span so that the second of the two terms on the right-hand side of Eq. (2) may be neglected. Since the component of momentum on the pressure side of the tip clearance convects through the tip gap almost unchanged and the suction and pressure sides of the blade are (to a first approximation) parallel, Eq. (2) may be rewritten

$$\Delta\xi = 2C_D L\left(\frac{\tau\Delta c}{sh\cos\alpha}\right)\left(1-\sqrt{\frac{P_{01}-P_P}{P_{01}-P_2}}\right) \tag{3}$$

Equation (3) shows that for a given blade, it is the discharge coefficient that primarily determines the overall cascade loss. In a different study, Yaras and Sjolander (1992) showed that a mixing model based on the kinetic energy rather than the momentum of the tip leakage flow also shows a linear dependency on C_D. Reducing the discharge coefficient will therefore tend to reduce the cascade loss. It should be noted that this loss includes the effect of the entropy gain over the tip: If there were no mixing within the tip gap the discharge coefficient would be equal to the contraction coefficient (0.611 for a sharp-edged orifice), whereas mixing increases the tip discharge coefficient to 0.844 (see Eq. (1)). The flux of loss of stagnation pressure from within the gap to the mainstream, $\Delta\xi_\tau$, caused by the complete mixing of the leakage flow with the wake of the vena contracta separation bubble, over a small part of the blade chord, Δc, may be expressed by Eq. (4):

$$\Delta\xi_\tau = \sqrt{\frac{\frac{1}{2}\rho V_{SN}^2}{P_{01}-P_2}}\left(\frac{P_P - P_S - \frac{1}{2}\rho V_{SN}^2}{P_{01}-P_{02}}\right)$$

$$= C_D(1-C_D^2)L^3\left(\frac{\tau\Delta c}{sh\cos\alpha_2}\right) \tag{4}$$

The Effects of the Blade Tip Geometry. *The Rounding of the Pressure Side Tip Corner.* The rounding of pressure side corners is known (McGreehan and Schotsch, 1988) to increase the size of the contraction coefficient. By doing so, the losses in the tip gap are reduced. But at the same time, the discharge coefficient is enhanced and it is this which determines the overall losses at cascade exit. Equation (3) indicates that the variation of the cascade loss, for a particular cascade at a single clearance, with contraction coefficient may be represented by the variation of C_D described by Eq. (1). Similarly, the variation of the losses generated within the tip gap with contraction coefficient for the same cascade may be plotted (from Eq. (4)) as the variation of $C_D(1-C_D^2)$. These are shown in Fig. 12. The curves clearly suggest that the designers of tip geometries should aim to decrease the value of the contraction coefficient σ, rather than increase it, even at the expense of increasing the loss production within the tip gap. This explains why the attempt of Bindon and Morphis (1992) to reduce the cascade losses by rounding the pressure side corner failed.

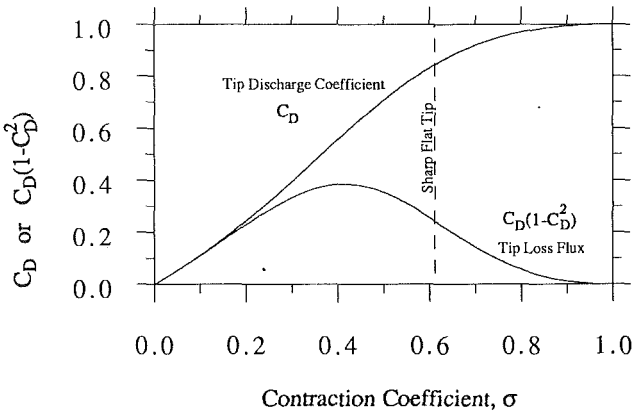

Fig. 12 The effect of contraction coefficient on the gap loss flux and discharge coefficient for a flat tip

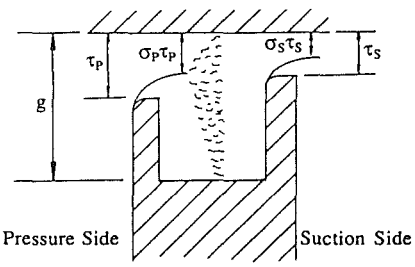

Fig. 13 Simple model for leakage flow over a tip with squealers

Suction and Pressure Side Squealers. If a squealer is fitted to a plain tip, the discharge coefficient will depend on the height of the squealer since this affects not only the contraction coefficient (Benson and Pool, 1965) but also the area change from the vena contracta to the tip gap exit. Figure 13 illustrates the one-dimensional incompressible calculation used to model the tip clearance. The flow is assumed to mix out fully after the pressure side squealer. This particular model also includes the effects of a suction side squealer. By assuming each vena contracta to be isentropic and by applying the conservation equations for mass and momentum between the squealers where the flow is considered to mix out, the discharge coefficient is found to be given by

$$C_D = \frac{1}{\left\{\left(1-\frac{2\tau_p\sigma_p}{g}\right)\left(\frac{\tau_S\sigma_S}{\tau_p\sigma_p}\right)^2 + \left(\frac{\tau_S\sigma_S}{g}\right)^2 + 1\right\}} \tag{5}$$

where the symbols are defined in Fig. 13.

According to Eq. (3) the ranking of tip geometries, on a particular clearance, essentially requires a calculation of their

Table 2. Summary of tip geometries

	Cascade A	Cascade B
Flat tip		
Radius / Chord (%)	0.3	0.0
Suction side Squealer		
Height / Chord (%)	6.75	1.0
Thickness / Chord (%)	0.34	0.73
Radius / Chord (%)	0.0	0.73
Pressure side Squealer		
Height / Chord (%)	6.75	1.0
Thickness / Chord (%)	0.35	0.73
Radius / Chord (%)	0.0	0.73

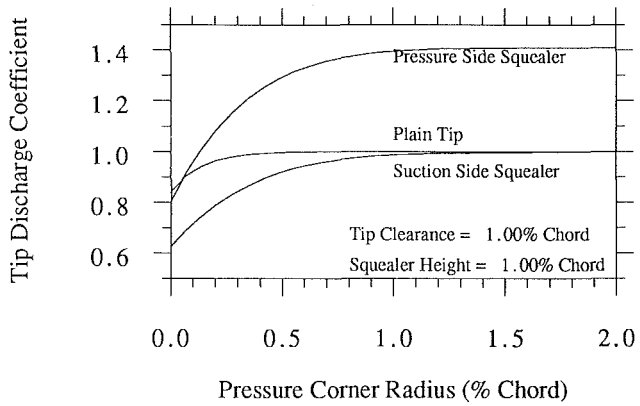

Fig. 14 Predicted variation of C_D with pressure corner radius

discharge coefficients. Using measured values of the blade pressure side corner radius, the radius of the squealers on their pressure sides and the height of the squealers as shown in Table 2 together with appropriate orifice flow correlations for the variation of σ with the rounding of the pressure side (McGreehan and Schotsch, 1988) and suction side squealer height (Benson and Pool, 1965), it is possible to rank the tested tip geometries. The results for the geometries of cascade A and B are plotted in Figs. 7(b) and 9(b). The actual value of the loss is not calculated since there is no allowance made for variation of tip loading, L, with clearance. The values of C_D appear over each histogram.

Comparing the predicted discharge coefficients with the measured cascade losses in Figs. 7 and 9, it is seen that the model correctly predicts the relative performance of the geometries in both cascades, despite the fact that the flat tip is measured to perform better than the squealers in cascade B and worse in cascade A. It reveals the advantage of the suction side squealer. This occurs because the vena contracta forms on the suction side of the tip gap and no mixing can occur within the clearance gap so that the contraction of the jet effectively blocks the leakage flow path.

Figure 14 shows the variation of the tip discharge coefficient for the three geometries as a function of the rounding of the pressure side corner of the blade tip or squealer, for squealer heights and tip clearances of 1 percent chord. The figure highlights the importance of the tolerances on the tip geometry. Advantages are to be gained from the pressure side squealer (assuming the model is correct in its assumption of complete mixing over the tip) only if the pressure side corner is sharp. For a blade tip with a one inch chord, a corner radius of one thousandth of an inch is sufficient to remove any aerodynamic advantage that a pressure side squealer might have over a plain, flat tip. On the other hand the suction side squealer shows a benefit over the flat tip even a quite large values of corner radius. (In this case the pressure side of the tip is rounded as well as the squealer pressure side.) In general, therefore, small-scale details of the geometries are vitally important to the aerodynamic gains to be expected from the addition of squealers. For the best performance of any geometry, the pressure side radii should be kept to a minimum.

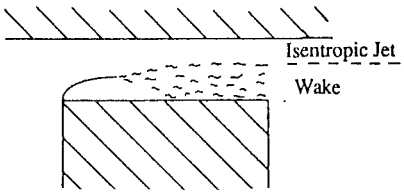

Fig. 15 Model for flow over a tip with partial mixing

The Effects of Incomplete Mixing in the Clearance Gap. The model described above has been used to analyze the performance of various tip geometries and has been shown to be qualitatively correct. Two of the main assumptions of the simple model were that mixing over the blade tip was completed before the leakage flow exited from the tip gap and that the leakage flow could be represented by parallel flow without curvature at the crest of the vena contracta, just prior to mixing. This section examines the first of these assumptions.

Bindon (1986) has reported tip gap exit velocity profiles at various chordwise positions for cascade A. His data show that rather than being completely mixed out, the flow at gap exit is characterized by a thin endwall boundary layer, a region of low total pressure loss in the middle of the gap, and a thick wake where the main leakage flow has started to mix after the vena contracta. These features are especially noticeable where the tip gap length is less than approximately five clearance heights. The hot-wire data of Fig. 10 also indicated that a nonuniform flow exists at gap exit.

In the model that follows, the tip gap exit flow will be represented by a combination of an isentropic jet and a wake, as shown in Fig. 15. The contribution of the bubble wake to the overall gap loss and therefore the discharge coefficient can be varied by varying the mixing coefficient M, which represents the fraction of the tip gap volume flow that mixes to form the bubble wake.

Given that isentropic flow occurs up to the vena contracta and that mass is conserved from there to gap exit, a simple relationship exists betweent the discharge coefficient and the static pressure coefficient in the separation bubble (the "bubble pressure coefficient"), which is defined as

$$C_{Pb}=\frac{P_P-P_b}{P_P-P_S} \tag{6}$$

so that

$$C_D=\sigma\sqrt{C_{Pb}} \tag{7}$$

Equation (7) is independent of the mixing processes and even the growth of an endwall boundary layer downstream of the vena contracta. Thus, we can obtain values for the contraction and mixing coefficients if we know the values of the bubble static pressure and the local discharge coefficient, both of which can be measured with relative ease.

Figure 16 shows the results of a series of calculations for a flat tip configuration. Dashed lines, representing different values of the mixing coefficient M (0 = no mixing; 1 = fully mixed out), are plotted on a graph of C_{Pb} against C_D. Lines of constant contraction coefficient are also shown. Although the value of M relies heavily on the assumed nature of the leakage flow, deductions can be made as to the nature of the flow, which corresponds to measured data. The results are valid for any value of pressure side corner radius since this only affects the contraction coefficient directly. It can be seen

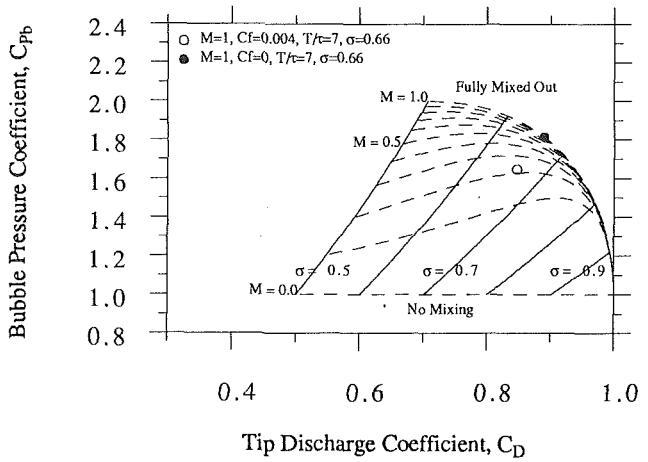

Fig. 16 Predicted effect of mixing upon the discharge and bubble pressure coefficients assuming no streamline curvature at the vena contracta

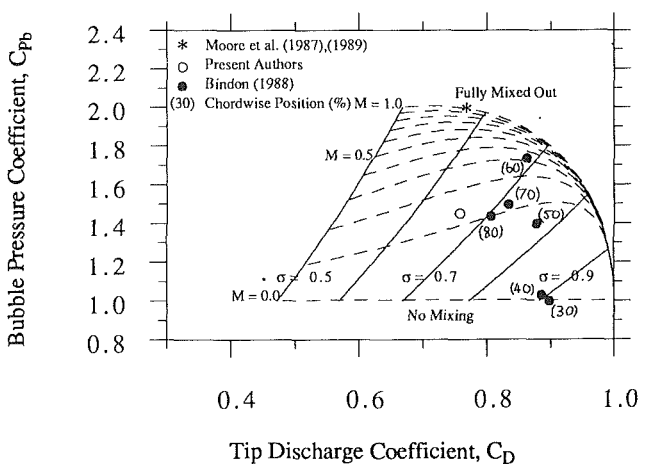

Fig. 17 Effect of mixing upon the discharge and bubble pressure coefficients allowing for curvature of the streamlines at the vena contracta

that for a given value of the contraction coefficient, any mixing that occurs over the tip between the jet and wake flows serves to increase the gap discharge coefficient and thus the expected loss for a given clearance. For example, the curve for $\sigma = 0.611$ shows that mixing over the tip can increase the discharge coefficient (and therefore the expected cascade loss) by 38 percent over that expected if no mixing were to occur. The mixing coefficient M is clearly an important parameter in this model, especially for low values of M.

Clearly the amount of mixing that occurs over the tip will depend on the Reynolds number of the tip clearance flow based on the distance that the tip leakage flow covers over the tip, T. The value of M is not necessarily constant for constant values of T/τ but in general, M is likely to increase as T/τ increases for a given cascade and tip geometry. As a result, the value of M and thus C_D will vary along the blade cord. If the value of σ is constant, then thick parts of the blade will be associated with higher values of C_D than thinner parts of the blade, if mixing is the dominant feature of the tip flow. On the other hand, shear stress on the endwall and blade tip will tend to reduce the mass flow as the blade thickness increases as discussed below.

The Effect of Boundary Layer Growth Over the Blade Tip. The model for the tip discharge coefficient in Eq. (1) assumes that there is no endwall or blade tip shear force. However, an estimate of the effect of such a force on the tip discharge coefficient may be made without difficulty. If the wall shear stress τ_w is assumed constant within the tip gap, then the force resisting the flow through the tip gap (per unit chord) is approximately $2\tau_w T$. The shear stress may be estimated from a characteristic dynamic head in the tip gap and a typical skin friction coefficient for turbulent flow

$$\tau_w = \frac{1}{2}\rho V_b^2 C_f \tag{8}$$

where V_b is the velocity at the crest of the vena contracta, and as such represents the maximum velocity in the tip gap. The value of C_f is taken to be 0.004.

Incorporating this model into that of Moore and Tilton, Eq. (1) is modified to give Eq. (9):

$$C_D = \frac{\sigma}{\sqrt{1 + 2C_f\frac{T}{\tau} - 2\sigma + 2\sigma^2}} \tag{9}$$

The reduction of discharge coefficient for a typical T/τ of 7 and contraction coefficient of 0.66 is 5 percent. Such a change plotted on Fig. 16 would indicate a reduction of the deduced value of M from 1.0 to 0.2. Clearly any deductions from Fig. 16 as to the nature of the leakage should be made with care.

The Effect of Flow Curvature at the Vena Contracta. It has so far been assumed that the velocity is constant across the vena contracta. However, a bubble of finite axial length will imply that there will be curvature of the streamlines near the bubble crest and a consequent variation in velocity as the curvature falls to zero at the endwall. Measurements to date (see Bindon, 1986, Moore and Tilton, 1988, and Fig. 10) have shown that the static pressure on the endwall over the mean contracta does not fall as far as the value in the separation bubble. Typically the ratio of the bubble pressure coefficient, C_{Pb} to the pressure coefficient on the endwall C_{pe}, defined in the same way as C_{Pb}, is 1.1. The effect of this pressure difference on the discharge coefficient is examined by assuming a model of the flow over the vena contracta.

In order to ascertain the size of the effect of local flow curvature on estimates of the discharge coefficient, a simplified model of the flow around the vena contracta is put forward. If it is assumed that the shape of the tip separation bubble is elliptical from tip gap entry to the bubble crest, then the length of the semiminor axis or the bubble height will be $(1 - \sigma)\tau$. The length of the semimajor axis or half the bubble length is assumed to be equal to 1.2τ, a value suggested by evidence presented by Graham (1985), Bindon (1986), Moore and Tilton (1988), and Moore et al. (1989). Assuming that the curvature of the streamlines varies linearly across the gap, reaching zero on the endwall, then an integration of the equation for radial equilibrium gives the ratio of C_{Pb} to C_{Pe} a value of 1.1 for contraction coefficient of 0.66. When the variation of velocity and static pressure across the gap is incorporated into the partial mixing model outlined above, Fig. 17 results. Experimental data from a variety of sources (Moore and Tilton, 1988, Bindon, 1989, Dishart and Moore, 1990, and Fig. 10) are also plotted. In effect, the discharge and bubble pressure coefficients reflect a higher value for σ than the value obtained without allowing for the flow curvature. Nevertheless the effect is small: The difference in C_D predicted by Fig. 17 for the fully mixed-out flow with a contraction coefficient of 0.66 is only 5 percent.

Comparison With Experimental Data. Bindon (1989) has reported discharge coefficients and tip pressure coefficients within the separation bubble deduced from his measurements in cascade A for a clearance equal to 2.5 percent chord. The

data for six chordwise positions are plotted in Fig. 17. Over the first half of the blade, the inferred contraction coefficients σ are relatively high, lying between 0.9 and 0.78. Also, the indicated values of the mixing coefficient M are relatively low given that the relative length of the leakage flow path is high at these locations ($T/\tau = 7.46$ at 30 percent chord; $T/\tau = 5.52$ at 50 percent). The reason for these relatively unexpected values of M is the growth of the endwall boundary layer inside the tip gap. Bindon's plots of blade tip static pressure at 30, 40, and 50 percent chord all exhibit a substantial *fall* in static pressure after the blade tip separation bubble reattaches. This is consistent with the action of endwall skin friction, and leads to a lowering of the discharge coefficient and the bubble pressure coefficient. The high value of σ observed is not yet fully understood. The effect is likely to be linked to the chordwise pressure gradients in these regions.

Over the second half of cascade A, Fig. 17 shows that using Bindon's data, the inferred σ remains at a constant value of approximately 0.70 but the value of M falls toward the trailing edge. This is the expected trend for changes in the flow being dominated by mixing rather than endwall shear; assuming that mixing rates are determined by the local Reynolds number based on the blade thickness, the degree of mixing at the tip gap exit should decrease as T/τ decreases. Here T/τ falls from 4.48 at 60 percent chord to 2.48 at 80 percent. The indicated value of M similarly falls from 0.35 to 0.1. At all locations, however, Fig. 17 indicates that the mixing is insubstantial and that the expected loss will consequently be lower than might be expected from a "fully mixed" calculation. Endwall and blade tip shear would have less of an effect on C_D as the blade thickness decreased toward the trailing edge.

The data taken from Bindon (1989) in Fig. 17 indicate a contraction coefficient of 0.7 for the second half of cascade A, which is close to the value of 0.72 predicted using the results of McGreehan and Schotsch (1988). The datum obtained by Moore and Tilton (1988) and Dishart and Moore (1990), which is plotted in Fig. 17, gives a low value of σ equal to 0.58 and indicates that in their measurements, the tip flow is almost fully mixed out. This mixing is due to the relatively long leakage path ($T/\tau = 7.3$), but the exceptionally low value of σ remains unexplained. The fact that the flow is almost fully mixed out explains the success of the simple model of Moore and Tilton (1988) (Fig. 1) in predicting the endwall and tip static pressures. The data shown in Fig. 10, reduced to a value of C_D and C_{Pb} and plotted on Fig. 17, yield a contraction coefficient of 0.66, higher than the value of 0.611 given by the potential flow solution, but equal to the value displayed on the measured velocity contours. The value of T/τ for this case is 3.3, very close to that of cascade A at 70 percent chord. Interestingly, the indicated values of the mixing coefficient M are also very close.

Conclusions

The effects of changing the tip geometry upon the performance of a linear cascade have been investigated in a linear cascade and by using simple one-dimensional flow models. The results have shown that the use of squealers, particularly suction side squealers, can provide a benefit over the flat tip.

The results obtained from the presented models confirm that, in principle, the designers of turbines should attempt to limit the mass flow through the tip gap at a given clearance rather than the loss generation over the tip. The models and data confirm that the radius of the corner from which the flow separates to form the vena contracta is vitally important and should be kept to a minimum to minimize the leakage flow.

It is found that in the majority of cases, the leakage jet flow that emerges from the tip gap is far from uniform and that as a result, the discharge coefficient can be significantly less than that predicted for the fully mixed-out case. Also, allowance for the curvature of the streamlines at the vena contracta and shear on the endwall and blade tip lead to a further decrease in the estimate of the leakage mass flow. The result is that the fully mixed-out model, although qualitatively correct, will overpredict the clearance loss.

References

Benson, R. S., and Pool, D. E., 1965, "The Compressible Flow Discharge Coefficients for a Two-Dimensional Slit," *Int. J. Mech. Sci.*, Vol. 7, pp. 337–353.

Bindon, J. P., 1986, "Pressure and Flow Field Measurements of Axial Turbine Tip Clearance Flow in a Linear Cascade," CUED/A-Turbo TR-123, Cambridge University, United Kingdom.

Bindon, J. P., 1989, "The Measurement and Formation of Tip Clearance Loss," ASME JOURNAL OF TURBOMACHINERY, Vol. 111, pp. 257–263.

Bindon, J. P., and Morphis, G., 1992, "The Development of Axial Turbine Leakage Loss for Two Profiled Tip Geometries Using Linear Cascade Data," ASME JOURNAL OF TURBOMACHINERY, Vol. 114, pp. 198–203.

Booth, T. C., Dodge, P. R., and Hepworth, H. K., 1982, "Rotor Tip Leakage: Part 1—Basic Methodology," ASME *Journal of Engineering for Power*, Vol. 104, pp. 154–161.

Booth, T. C., 1985, "Turbine Loss Correlations and Analysis," VKI Lecture Series 1985-05, *Tip Clearance Effects in Turbomachines*.

Denton, J. D., and Cumpsty, N. A., 1987, "Loss Mechanisms in Turbomachines," Proc. IMechE, *Turbomachinery—Efficiency and Improvement*, Paper No. C260/87.

Dishart, P. T., and Moore, J., 1990, "Tip Leakage Losses in a Linear Turbine Cascade," ASME JOURNAL OF TURBOMACHINERY, Vol. 112, pp. 599–608.

Graham, J. A. H., 1985, "Investigation of a Tip Clearance Cascade in a Water Analogy Rig," ASME Paper No. 85-IGT-65.

Hodson, H. P., 1983, "The Development of Unsteady Boundary Layers on the Rotor of an Axial Flow Turbine," *Viscous Effects in Turbomachines*, ADARD CP-351, Copenhagen.

Hodson, H. P., and Addison, J. S., 1989, "Wake-Boundary Layer Interactions in an Axial Flow Turbine Rotor at Off-Design Conditions," ASME JOURNAL OF TURBOMACHINERY, Vol. 111, pp. 181–192.

Kicks, J. C., 1970, "Development and Refinement of an Ultraminiature Pressure Transducer and Application to Airplane Model and Airplane Subsystem Testing in Wind Tunnels," *Proc. 6th International Aerospace Symposium*, Cranfield, United Kingdom, pp. 9.1–9.18.

McGreehan, W. F., and Schotsch, M. J., 1988, "Flow Characteristics of Long Orifices With Rotation and Corner Radiusing," ASME JOURNAL OF TURBOMACHINERY, Vol. 110, pp. 213–217.

Milne-Thomson, L. M., 1968, *Theoretical Hydrodynamics*, 5th ed., MacMillan & Co. Ltd., pp. 310–311.

Moore, J., and Tilton, J. S., 1988, "Tip Leakage Flow in a Linear Turbine Cascade," ASME JOURNAL OF TURBOMACHINERY, Vol. 110, pp. 18–26.

Moore, J., Moore, J. G., Henry, G. S., and Chaudhry, U., 1989, "Flow and Heat Transfer in Turbine Tip Gaps," ASME JOURNAL OF TURBOMACHINERY, Vol. 111, pp. 301–309.

Rains, D. A., 1954, "Tip Clearance Flows in Axial Flow Compressors and Pumps," CIT Hydro. and Mech. Eng. Labs, Report No. 5.

Rayleigh, J. W. S., 1876, "Notes on Hydrodynamics," Scientific Papers, Vol. 1; Dover Publications, 1964, pp. 297–304.

Wadia, A. R., and Booth, T. C., 1981, "Rotor Tip Leakage: Part 2—Design Optimization Through Viscous Analysis and Experiment," ASME Paper No. 81-GT-XX.

Yaras, M. I., and Sjolander, S. A., 1992, "Prediction of Tip-Leakage Losses in Axial Turbines," ASME JOURNAL OF TURBOMACHINERY, Vol. 114, pp. 204–210.